Journal of Non-Newtonian Fluid Mechanics 260 (2018) 101–108

Contents lists available at ScienceDirect

Journal of Non-Newtonian Fluid Mechanics

journal homepage: www.elsevier.com/locate/jnnfm

Determining true material constants of viscoplastic materials from rotational rheometer data

Andreas N. Alexandrou[a,*], Georgios C. Georgiou[b,*], Eva-Athena Economides[a], Christoph Zang[c], Michael Modigell[c]

[a] Department of Mechanical and Manufacturing Engineering, University of Cyprus, PO Box 20537, Nicosia 1678, Cyprus
[b] Department of Mathematics and Statistics, University of Cyprus, PO Box 20537, Nicosia 1678, Cyprus
[c] Department of Mechanical Engineering University of Aachen, Aachen, Germany

ARTICLE INFO

Keywords:
Viscoplastic materials
Rheometry
Couette rheometer
Herschel–Bulkley fluids
Material constants

ABSTRACT

We analyse the circular Couette flow of Herschel–Bulkley fluids to investigate the validity of the assumption that the rate of strain distributions across the gap share a common point. It is demonstrated that this is true only with fully-yielded Bingham -plastic flow. In other cases, e.g., in partially-yielded Bingham-plastic flow or fully-yielded Herschel–Bulkley flow, the common point for the fully-yielded Bingham case provides a good approximation for determining material constants only if the gap is sufficiently small. We also revisit the important issue of determining material properties of viscoplastic fluids by using "true values" for the rate of strain and demonstrate that the material properties can be very different from those obtained using "apparent' values for the rate of strain.

1. Introduction

The main objective in viscometry is to determine *objectively* fluid material constants independent of experimental and analysis errors. In principle, these material constants are determined by curve fitting using the measured values of stress and the rate of strain. However, in complex fluids, the rate of strain depends on both the velocity distribution and the material constants whose values of course are unknown and they are the objective of the analysis. Unfortunately, only in very few cases the velocity distribution is both known *a priori* and independent of the material constants. Traditionally then the velocity distribution is taken from the analytical solution of an *a priori* assumed constitutive model, such as the Newtonian or the power-law models. It turns out however that the rate of strain calculated using the predicted material constants is usually different from the initially assumed rate. This is because the initially assumed constitutive model for an arbitrary fluid is not necessarily the same as that determined by the experiments. For example, one can assume initially a Newtonian behavior to end up predicting a Herschel–Bulkley flow curve! Therefore, analyses where the rheology is assumed *a priori* can only yield "apparent" and not "true" material constants. As shown in [1] the introduced error in viscoplastic fluids can be significant. In the present work, by using data for typical viscoplastic fluids we demonstrate this fact and explain in detail of how "true" material parameters can be obtained.

In the following sections, we summarize already available analytical solutions for the circular Couette flow of Herschel–Bulkley materials and discuss the existence of common intersection points. Then, we analyze the flow in the general case and propose a systematic method for the determination of the material constants of Herschel–Bulkley fluids. We focus on an interesting approach proposed by Schummer and Worthoff [3] where in viscometric flows flow curves can intersect at a common point within the rheometer whose location is independent of the rheology of the fluids. Schummer and Worthoff [3] demonstrated this concept for a number of flows and found approximate locations where the resulting experimental error is minimum. Obviously, this is a profound result because one can experimentally get "true" material constants without iteration or other corrections. We investigate this concept for the case of Herschel–Bulkley fluids in a rotational rheometer whose basic flow is represented by the classical circular-Couette flow. The general problem of the rate of strain being a function of the material constants can be resolved by proper iteration between the experimental data and the predicted model parameters [2]. Finally, the method is applied to available data for a cosmetic emulsion and a coal-water mixture. To our knowledge, this is the first time that comparisons between true and apparent values of the rheological parameters are made. For the particular experimental data, the relative errors in the consistency index, the power-law exponent, and the yield stress are found to be high, moderate, and very small, respectively.

* Corresponding author.
E-mail addresses: andalexa@ucy.ac.cy (A.N. Alexandrou), georgios@ucy.ac.cy (G.C. Georgiou).

https://doi.org/10.1016/j.jnnfm.2018.07.002
Received 16 February 2018; Received in revised form 14 April 2018; Accepted 10 July 2018
0377-0257/

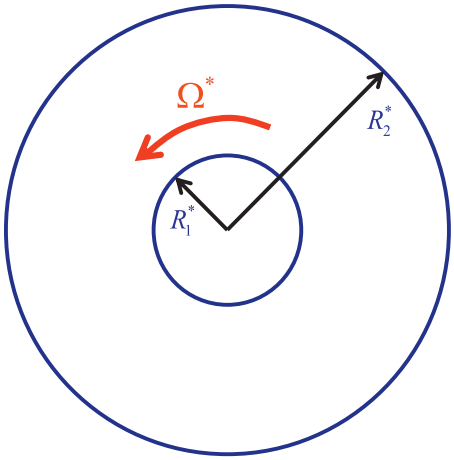

Fig. 1. Schematic of the geometry of the flow.

2. Theoretical framework

Let us consider the steady flow of a viscoplastic material between two co-axial, infinitely long cylinders of radii R_1^* and R_2^*, where $R_2^* > R_1^*$. It should be noted that throughout this work the stars denote dimensional quantities. Symbols without stars will denote dimensionless variables and parameters. The inner cylinder is rotating at a constant speed Ω^* while the outer cylinder is fixed, as illustrated in Fig. 1. The solution of this flow can be found in the literature (see, e.g., [1]). It is thus conveniently summarized here in order to provide the theoretical basis for the determination of "real" material constants and to illustrate the range of validity of the assumption that there is a common point independent of the fluid rheology.

Under the assumption of axisymmetric flow only in the azimuthal direction, the conservation of linear momentum for any fluid yields

$$\tau_{r\theta}^* = \frac{c^*}{r^{*2}} \tag{1}$$

and the rate of strain is given by

$$\dot{\gamma}^* = r^* \left| \frac{d}{dr^*}\left(\frac{u_\theta^*}{r^*}\right)\right| = -r^* \frac{d}{dr^*}\left(\frac{u_\theta^*}{r^*}\right) \tag{2}$$

The constitutive equation for a Herschel–Bulkley fluid may be written in scalar form as follows:

$$\begin{cases} \dot{\gamma}^* = 0, & \tau^* \le \tau_0^* \\ \tau^* = \tau_0^* + k^* \dot{\gamma}^{*n}, & \tau^* > \tau_0^* \end{cases} \tag{3}$$

where $\tau^* = |\tau_{r\theta}^*|$, τ_0^* is the yield stress, n is the power-law exponent, and k^* is the consistency index. The above model is a combination of the Bingham-plastic model ($n=1$) and the power-law model ($\tau_0^* = 0$). The Newtonian fluid corresponds to $n=1$ and $\tau_0^* = 0$.

In what follows, we will work with non-dimensionalized equations. The dimensionless variables are defined by

$$u_\theta \equiv \frac{u_\theta^*}{\Omega^* R_1^*}, \quad r \equiv \frac{r^*}{R_1^*}, \quad \dot{\gamma} \equiv \frac{\dot{\gamma}^*}{\Omega^*}, \quad \tau \equiv \frac{\tau^*}{\tau_0^*} \tag{4}$$

With the above scalings, the dimensionless form of the constitutive equation (3) is

$$\begin{cases} \dot{\gamma} = 0, & \tau \le 1 \\ \tau = 1 + \frac{1}{Bn}\dot{\gamma}^n, & \tau > 1 \end{cases} \tag{5}$$

where

$$Bn \equiv \frac{\tau_0^*}{k^* \Omega^{*n}} \tag{6}$$

is the Bingham number. Combining Eqs. (1) and (5), the non-dimensional rate of strain in the yielded regime ($\tau > 1$) is given by

$$\dot{\gamma} = Bn^{1/n}\left(\frac{c}{r^2} - 1\right)^{1/n} \tag{7}$$

where $c \equiv c^*/R_1^{*2}\tau_0^*$. To obtain the velocity u_θ^* one simply needs to integrate and apply the boundary conditions. Below a certain critical Bingham number, Bn_{crit}, the fluid is yielded everywhere in the gap $1 \le r \le R_2$. In this case the boundary conditions are $u_\theta(1) = 1$ and $u_\theta(R_2) = 0$ (no-slip boundary conditions), which lead to the following expression for the velocity

$$u_\theta(r) = r\left[1 - Bn^{1/n}\int_1^r \frac{1}{\xi}\left(\frac{c}{\xi^2} - 1\right)^{1/n} d\xi\right], \quad 1 \le r \le R_2 \tag{8}$$

where the constant c is calculated by demanding that

$$Bn^{1/n}\int_1^{R_2} \frac{1}{\xi}\left(\frac{c}{\xi^2} - 1\right)^{1/n} d\xi = 1 \tag{9}$$

Above the critical value Bn_{crit}, the fluid is yielded only partially in the range $1 < r < r_0$, where $r_0 < R_2$ is the radial distance from the inner cylinder to the point where $\tau = |\tau_{r\theta}| = 1$. From Eq. (7) it is deduced that

$$c = r_0^2 \tag{10}$$

and therefore

$$\dot{\gamma} = \begin{cases} Bn^{1/n}\left(\frac{r_0^2}{r^2} - 1\right)^{1/n}, & 1 \le r \le r_0 \\ 0, & r_0 \le r \le R_2 \end{cases} \tag{11}$$

and

$$u_\theta(r) = \begin{cases} r\left[1 - Bn^{1/n}\int_1^r \frac{1}{\xi}\left(\frac{r_0^2}{\xi^2} - 1\right)^{1/n} d\xi\right], & 1 \le r \le r_0 \\ 0, & r_0 \le r \le R_2 \end{cases} \tag{12}$$

where r_0 is a root of

$$Bn^{1/n}\int_1^{r_0} \frac{1}{\xi}\left(\frac{r_0^2}{\xi^2} - 1\right)^{1/n} d\xi = 1 \tag{13}$$

3. Special solutions when $1/n$ is an integer

For selected values of n, i.e. $n=1$, 1/2, 1/3 etc., the equations used in the general case can be integrated analytically [1].

3.1. The Bingham plastic case ($n=1$)

For a Bingham plastic ($n=1$) it turns out that for $Bn > Bn_{crit}$,

$$u_\theta(r) = r\left[1 - Bn\left\{\frac{r_0^2}{2}\left(1 - \frac{1}{r^2}\right) - \ln r\right\}\right], \quad 1 \le r \le r_0 \tag{14}$$

and

$$\dot{\gamma} = Bn\left(\frac{r_0^2}{r^2} - 1\right), \quad 1 \le r \le r_0 \tag{15}$$

where r_0 is a root of

$$Bn = \frac{2}{r_0^2 - 2\ln r_0 - 1} \tag{16}$$

Obviously, the critical Bingham number Bn_{crit} above which the flow is partially yielded is:

$$Bn_{crit} = \frac{2}{R_2^2 - 2\ln R_2 - 1} \tag{17}$$

It is instructive to plot Bn_{crit} versus the outer radius R_2, as in Fig. 2. The critical Bingham number increases exponentially with the rheometer gap ($R_2 - 1$). When the dimensionless gap is 0.01 ($R_2 = 1.01$) the critical Bingham number is so high ($Bn_{crit} = 10033$) that one can safely assume that the flow is fully yielded for all non-exotic viscoplastic materials. However, if the gap is big the critical Bingham number is low and the possibility of having partially yielded flow cannot be excluded. For example, $Bn_{crit} = 103.2$ and 26.54 when $R_2 = 1.1$ and 1.2, respectively.

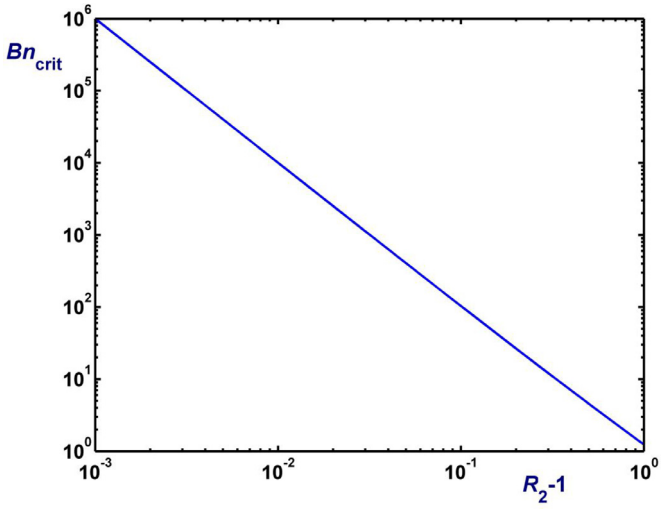

Fig. 2. Variation of the critical Bingham Bn_{crit} beyond which the flow is partially yielded with the dimensionless rheometer gap $(R_2 - 1)$.

For $Bn \le Bn_{crit}$ (fully-yielded flow) the velocity is given by

$$u_\theta(r) = r\left[1 + Bn\ln r - \frac{1 + Bn\ln R_2}{(1 - 1/R_2^2)}\left(1 - \frac{1}{r^2}\right)\right], \quad 1 \le r \le R_2 \tag{18}$$

Hence, the shear rate is

$$\dot\gamma = r\left|\frac{d}{dr}\left(\frac{u_\theta}{r}\right)\right| = 2\frac{1 + Bn\ln R_2}{(1 - 1/R_2^2)r^2} - Bn, \quad 1 \le r \le R_2 \tag{19}$$

It is easily verified that the critical radius r_c at which $d\dot\gamma/dBn = 0$ is

$$r_c = R_2\sqrt{\frac{2\ln R_2}{R_2^2 - 1}} \tag{20}$$

By substituting into Eq. (19) one finds that the corresponding rate of strain is

$$\dot\gamma_c = \frac{1}{\ln R_2} \tag{21}$$

At this point the shear rate is independent of the Bingham number. By setting $Bn = 0$ in Eqs. (18) and (19) the Newtonian expressions are recovered. It should be noted, however, that in this case a scaling different from that of Eq. (4) should be used for the shear stress.

The variation of r_c with the dimensionless gap $(R_2 - 1)$ is illustrated in Fig. 3. For very small gap sizes, i.e. $(R_2 - 1) < 0.1$ this point essentially coincides with the mean radius in the gap, r_m. As the gap size is increased, the common point moves closer to the rotating inner cylinder.

3.2. The case for $n = 1/2$

Even though the solutions for $n = 1/2$ and $1/3$ are provided in [1], we repeat the former here for convenience. When $n = 1/2$, the critical Bingham number is found to be given by

$$Bn_{crit} = \frac{2}{\sqrt{R_2^4 - 4R_2^2 + 4\ln R_2 + 3}} \tag{22}$$

For $Bn > Bn_{crit}$ (partially-yielded flow),

$$u_\theta(r) = r\left[1 - Bn^2\left\{\ln r - r_0^2\left(1 - \frac{1}{r^2}\right) + \frac{r_0^4}{4}\left(1 - \frac{1}{r^4}\right)\right\}\right], \quad 1 \le r \le r_0 \tag{23}$$

and

$$\dot\gamma = Bn^2\left(\frac{r_0^2}{r^2} - 1\right)^2, \quad 1 \le r \le r_0 \tag{24}$$

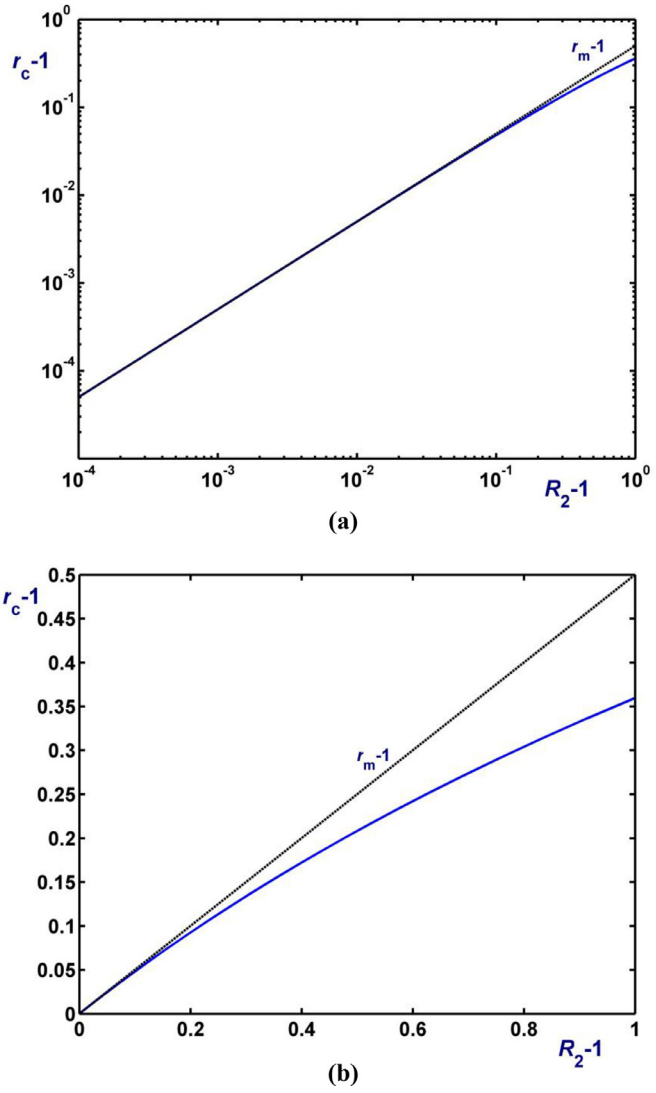

Fig. 3. Variation of r_c with the dimensionless rheometer gap $(R_2 - 1)$: (a) logarithmic plot; (b) linear plot; r_m is the radius corresponding to the middle of the gap.

where r_0 is a root of

$$Bn^2 = \frac{4}{r_0^4 - 4r_0^2 + 4\ln r_0 + 3} \tag{25}$$

For $Bn \le Bn_{crit}$ (fully-yielded flow), the velocity and the shear rate are respectively given by

$$u_\theta(r) = r\left[1 - Bn^2\left\{\ln r - c\left(1 - \frac{1}{r^2}\right) + \frac{c^2}{4}\left(1 - \frac{1}{r^4}\right)\right\}\right], \quad 1 \le r \le R_2 \tag{26}$$

and

$$\dot\gamma = Bn^2\left(\frac{c}{r^2} - 1\right)^2, \quad 1 \le r \le r_2 \tag{27}$$

where

$$c = \frac{2R_2^2}{1 + R_2^2}\left[1 + \sqrt{1 + \frac{1 + R_2^2}{1 - R_2^2}\left(\ln R_2 - \frac{1}{Bn^2}\right)}\right] \tag{28}$$

4. Discussion of common intersection points

As already mentioned, in the case of a Bingham plastic $(n = 1)$, the rate of strain distributions within the rheometer gap share a common

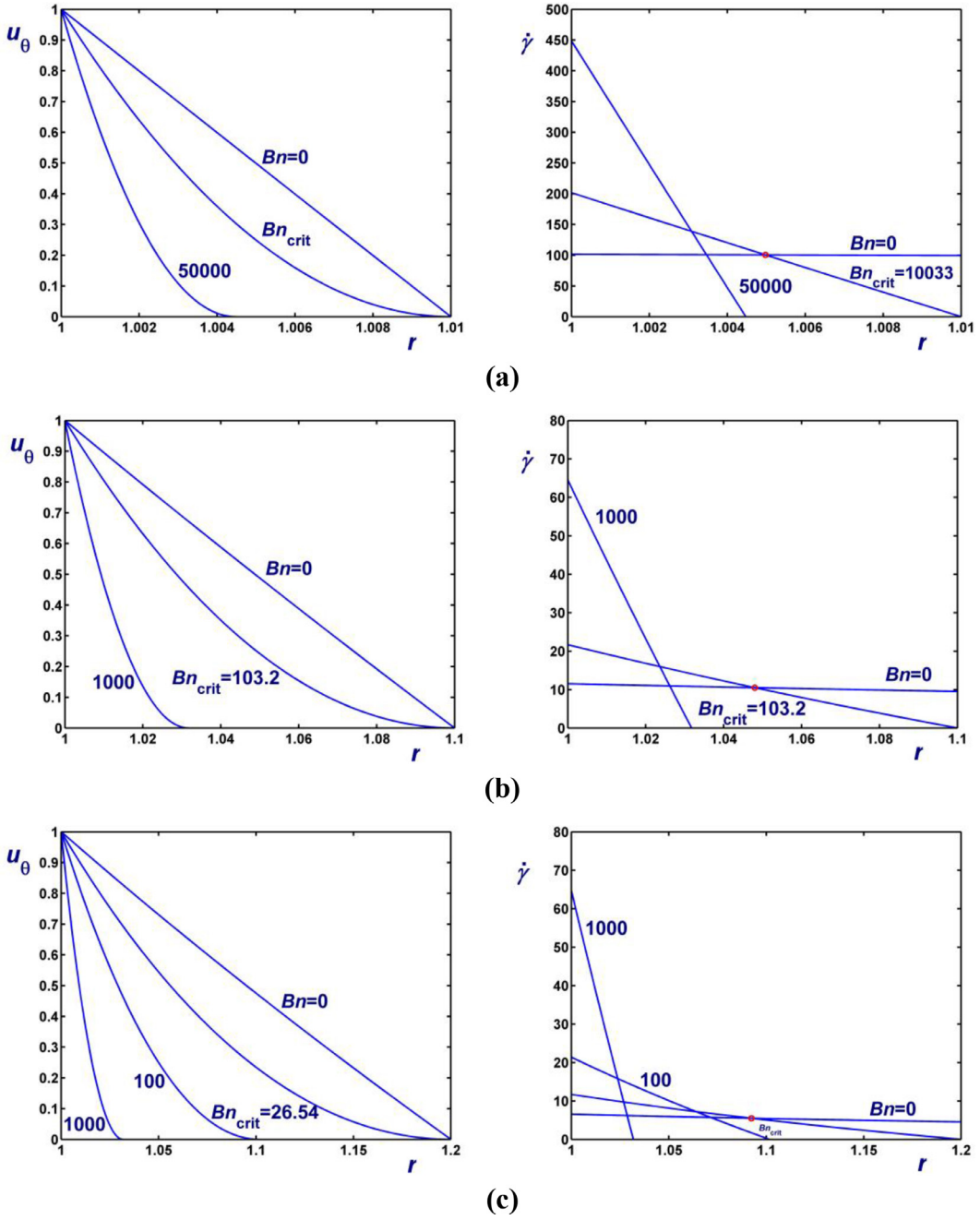

Fig. 4. Angular velocities and rates of strain for various Bingham plastics ($n=1$) for various radii ratios: (a) $R_2 = 1.01$ ($Bn_{crit} = 10033$); (b) $R_2 = 1.1$ ($Bn_{crit} = 103.2$); $R_2 = 1.2$ ($Bn_{crit} = 26.54$). The red circle corresponds to the common point that exists for $0 \le Bn \le Bn_{crit}$. (For interpretation of the references to colour in this figure legend, the reader is referred to the web version of this article.)

point that is independent of the Bingham number as long as the material within the rheometer is fully yielded, i.e. there are no solid-like regions ($Bn \le Bn_{crit}$). Fig. 4 shows velocity and rate of strain distributions for three different gap sizes, i.e. $R_2 = 1.01$, 1.1 and 1.2. As the outer radius is increased, the fixed point moves from the mid-radius towards the inner cylinder. For example, $r_c = 1.00498$, 1.04802 and 1.09242 when $R_2 = 1.01$, 1.1 and 1.2, respectively. The corresponding values of $\dot\gamma_c$ are 100.5, 10.49, and 5.485. It should be noted that when $Bn > Bn_{crit}$ the yield point r_0 eventually becomes less than r_c. In other words, there may not be even flow at the "common" point.

The results obtained for a representative Herschel–Bulkley fluid with $n = 0.5$ and $R_2 = 1.01$, 1.1 and 1.2 are shown in Fig. 5. The results are similar to those for the Bingham case ($n = 1$), the only difference being that the rate of strain distributions do not share a common point. This is illustrated in Fig. 6 for the case $R_2 = 1.1$.

Let us now consider the relative error when using the common point r_c for calculating the rate of strain rate. This is defined as

$$error = 100\left|\frac{\dot\gamma_a - \dot\gamma_c}{\dot\gamma_a}\right| \tag{29}$$

where $\dot\gamma_a$ is the actual the rate of strain, and $\dot\gamma_c$ is the rate of strain evaluated at r_c. In the case of a Bingham fluid ($n = 1$) the relative error is obviously zero when $Bn \le Bn_{crit}$ and non-zero when $Bn > Bn_{crit}$, i.e. when the flow is partially yielded. Moreover, for Bingham numbers greater

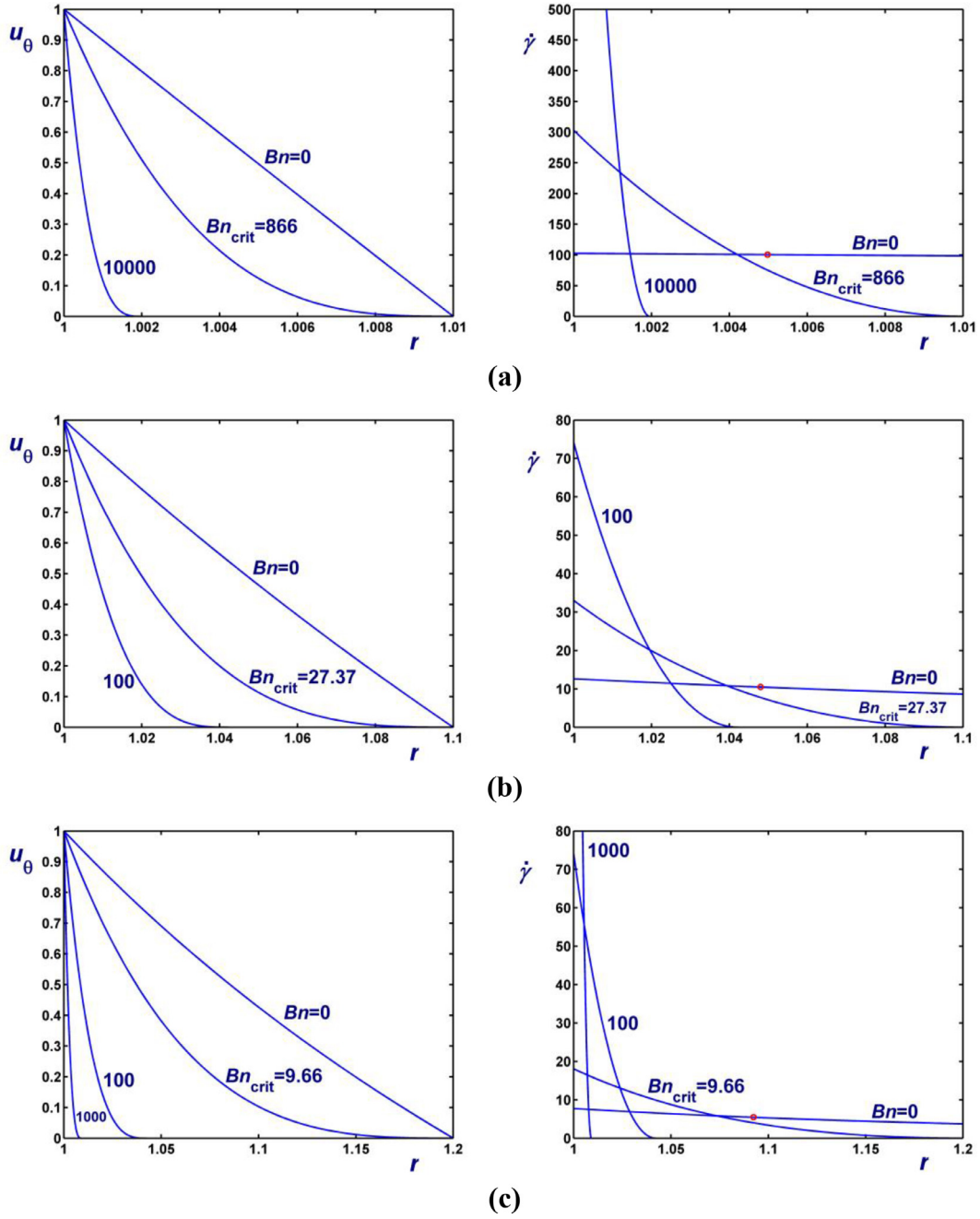

Fig. 5. Angular velocities and rates of strain for various Herschel–Bulkley fluids with $n = 0.5$ for various radii ratios: (a) $R_2 = 1.01$; (b) $R_2 = 1.1$; $R_2 = 1.2$. The red circle corresponds to the common point that exists in the case of fully-yielded Bingham flow. (For interpretation of the references to colour in this figure legend, the reader is referred to the web version of this article.)

than a second critical value,

$$Bn'_{crit} = \frac{2}{r_c^2 - 2\ln r_c - 1} > Bn_{crit} \tag{30}$$

the flow is unyielded at r_c and therefore the relative error defined above becomes infinite. The effects of Bn and R_2 on the relative error are illustrated in Figs. 7 and 8. In Fig. 7, the relative errors for $R_2 = 1.01$, 1.1 and 1.2 are plotted versus the Bingham number in the intervals $[Bn_{crit}, Bn'_{crit}) = [10{,}033{,}40{,}401)$, [103.2, 440.6), and [26.54, 120.6), respectively. When $Bn \le Bn_{crit}$ the error is, of course, zero. As already mentioned, Bn_{crit} is a decreasing function of R_2. For $Bn > Bn_{crit}$ the error increases rapidly becoming infinite as the Bingham number tends to Bn'_{crit}. In Fig. 8, the relative errors for $Bn = 1$, 10, and 100 are plotted versus the gap (R_2-1). For relatively small Bn and R_2^* the error can be very small, well below other experimental errors. R_2 appears to have a more pronounced effect: for small values of R_2 the error is rather small, even for large values of Bn.

The relative error becomes bigger for different values of the power-law exponent. For example, when for $n = 0.5$, the second critical Bingham number is given by

$$Bn'_{crit} = \frac{2}{\sqrt{r_c^4 - 4r_c^2 + 4\ln r_c + 3}} \tag{31}$$

and the corresponding intervals for the Bingham number for $R_2 = 1.01$, 1.1 and 1.2 are $[Bn_{crit}, Bn'_{crit}) = [866.0{,}2465)$, [27.37,82.30), and [9.658,30.81), respectively. In this case, there is no common point

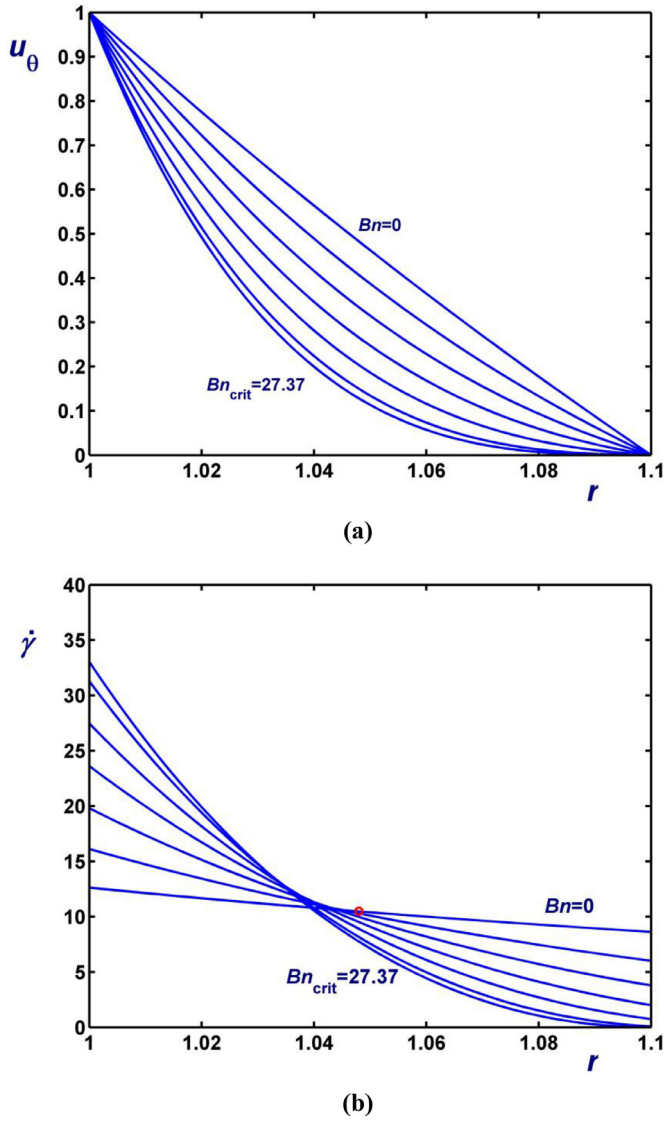

Fig. 6. Angular velocities (a) and rates of strain (b) in the fully-yielded regime for various Herschel–Bulkley fluids with $n = 0.5$ and $Bn = 0$, 5, 10, 15, 20, 25, and 27.37 when $R_2 = 1.1$. The red circle corresponds to the common point that exists in the case of fully-yielded Bingham flow. (For interpretation of the references to colour in this figure legend, the reader is referred to the web version of this article.)

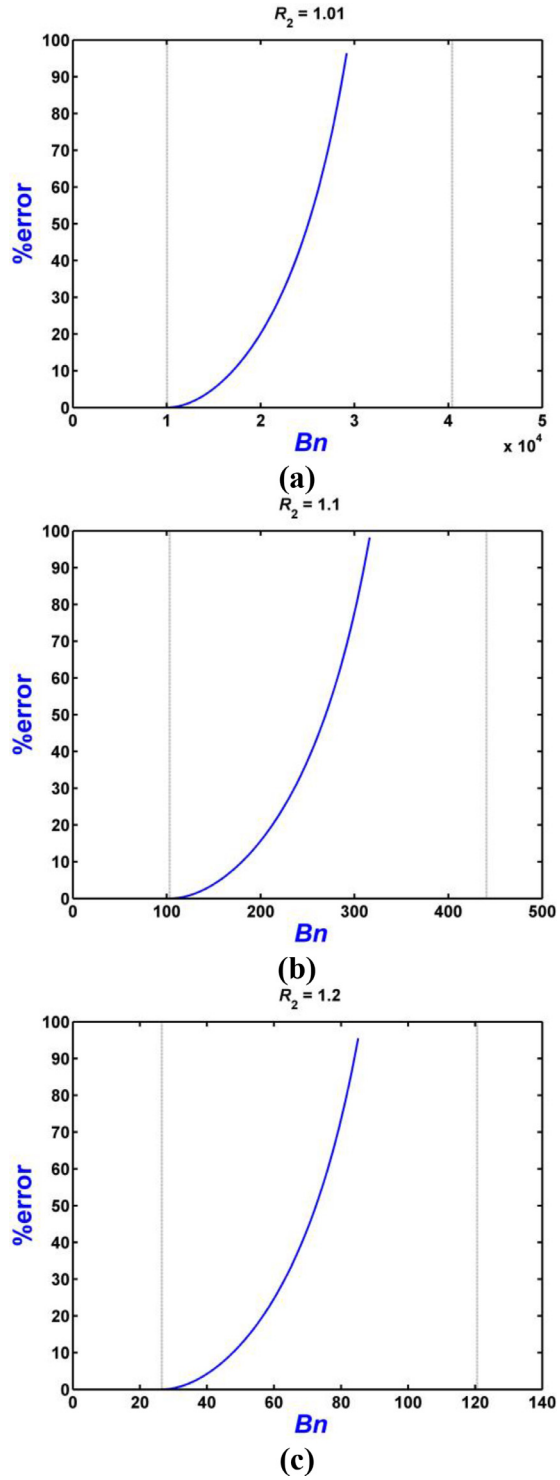

Fig. 7. Calculated error versus the Bingham number for $n = 1$ (Bingham fluid) and (a) $R_2 = 1.01$; (b) $R_2 = 1.1$; (c) $R_2 = 1.2$. The first vertical line corresponds to the critical Bingham number Bn_{crit} below which the flow is fully yielded. The second vertical line corresponds to the critical Bingham number at which the radius of the yielded region coincides with r_c.

when the flow is fully yielded and hence the error is non-zero even for $Bn \le Bn_{crit}$. In general, the relative error increases as n is reduced.

In an actual experiment then in order to use the concept of a common point we must first use Eq. (1) to get $c^* = R_1^{*2}/\tau_{w1}^*$ where τ_{w1}^* is the shear stress at the inner cylinder, obtained from the measured toque, as explained below. Therefore, the local stress at the common point r_c^* is calculated as

$$\tau_c^* = \tau_{w1}^* \frac{R_1^{*2}}{r_c^{*2}} \tag{32}$$

The significance of having a common intersection point is that the local rate of strain $\dot{\gamma}_c^*$ can be calculated using the Bingham plastic constitutive relation. The flow curve $(\tau_c^*, \dot{\gamma}_c^*)$ can be constructed by varying the rotational speed on the inner cylinder. The rheological parameters can then be obtained by means of nonlinear regression. As long as the material is Bingham plastic and the corresponding flow is fully yielded, the evaluated constants are the "true" material constants and no additional corrections are needed. In all other cases, the relative error in $\dot{\gamma}_c^*$, is of course, non-zero and additional corrections may be needed.

5. The general case

In the general case, such as when the theory is used to analyze actual experimental data, where the exponent $1/n$ is not an integer,

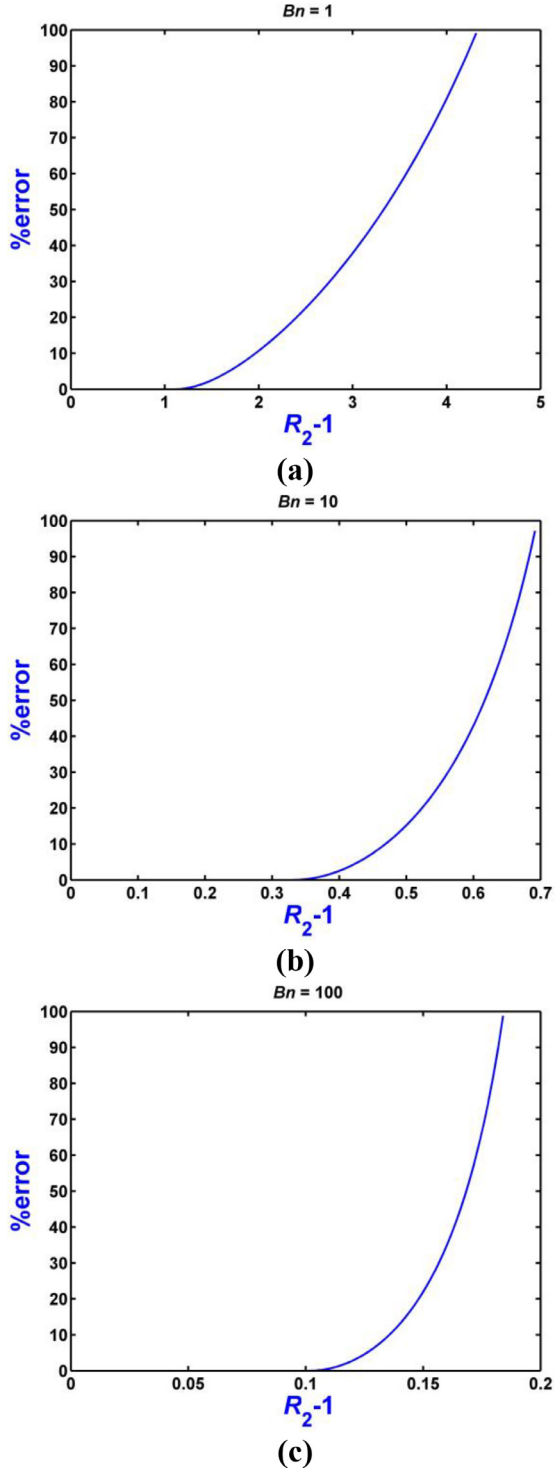

Fig. 8. Calculated error versus the gap (R_2-1) for $n=1$ (Bingham fluid): (a) $Bn=1$; (b) $Bn=10$; (c) $Bn=100$. The vertical lines indicate the maximum outer radius R_{2m} for which the material is fully yielded for each Bingham number (2.1226, 1.3313, and 1.1016, respectively).

Eqs. (8) and (9) or Eqs. (12) and (13) in the case of partial yielding, must be integrated numerically (there is no closed-form analytical solution when $1/n$ is not an integer).

The procedure to determine "true" material constants consistent with the theory involves four obvious major **steps**: (i) the solution of the boundary condition Eq. (9) (or Eq. (13) when we have partial yielding) in order to compute the unknown constant c or r_0; (ii) the evaluation/update of the rate of strain at the surface of the rotating cylinder for each rotational speed using Eq. (7); (iii) the evaluation of the yield stress τ_0^* by extrapolating linearly to the zero rate of strain; and (iv) the curve fitting using the yield stress τ_0^*, the measured stress and the constructed rate of strain for each value of Ω^* to obtain new values for the material constants, k^* and n. The four steps are repeated until all material constants converge up to eight significant digits.

In principle, all four steps are straightforward to complete and one can use a number of different numerical schemes. Here, step (i) was implemented using a combination of Simpson's integration and a Newton-Raphson iteration procedure for fast convergence of the non-linear equation. During this step care must be exercised to integrate the correct condition (Eq. (13) when partial yielding occurs). The curve fitting (step (iv)) was implemented using least squares either by solving the non-linear equation with the bi-section method or by solving directly the linearized form of the equation obtained by taking the log of the model equation. Below we apply and compare the results using both approaches.

The above procedure was tested on a number of different samples exhibiting viscoplastic behavior. Here we have chosen data on a cosmetic emulsion (dm, Balea Bodycremeocos sold by GmbH + Co. KG), obtained using a Searle-type rotational rheometer MCR501 by Anton Paar. The cup and rotational bob was made up with stainless steel. Reverting back to dimensional quantities, the radius of the bob was $R_1^*=11$ mm and that of the cup $R_2^*=13$ mm, while the length of the concentric cylinders was $L^*=20$ mm.

The experiments were conducted at a sample temperature of 25°C. A volume of 9 ml from the sample was filled into the cup, the bob was immersed into the sample until the tip reached a distance of 3 mm from the bottom. A conditioning period of 300 s was conducted with rotational speed of 5 1/s. After this, the torque was continuously increased from 0 to 1.5 Nm over 120 s.

Conventionally the rate of strain is evaluated using the results of Schümmer and Worthoff [3] who have suggested that there is a representative point r_c^* between R_1^* and R_2^*, where the shear stress and the shear rate for a pseudoplastic material are equal to those for a Newtonian fluid with only a small error. This method was used here to evaluate the stress and the strain rate from torque and rotational speed data. In the result shown below these data are referred to as *raw data.* The shear rate and the stress are calculated by means of

$$\dot{\gamma}_c^* = \frac{2\Omega^*}{1-\beta}\left(\frac{R_1^*}{r_c^*}\right)^2 \tag{33}$$

and

$$\tau_c^* = \frac{M^*}{2\pi L^* r_c^{*2} c_e^*} \tag{34}$$

where M^* is the measured torque,

$$\beta \equiv \left(\frac{R_1^*}{R_2^*}\right)^2 = \frac{1}{R_2^2} \tag{35}$$

and c_e^* is a correction factor for end effects [4]. The iterative solution for the true material constants employed here uses the stress τ_i^* at the inner cylinder and the angular velocity Ω^* as input.

Fig. 9 shows a comparison between the *raw data* and the data once the rate of strain has been corrected using the actual rheological parameters obtained from the curve fitting applied to the linear version of the least square equation. Table 1 shows the parameters and the relative

Table 1
Comparison between raw and corrected data.

	Corrected data	Raw data	Relative % error
τ_0^* (Pa)	50.34	50.69	0.690
k^* (Pa s^n)	37.10	50.08	34.99
N	0.308	0.278	9.74

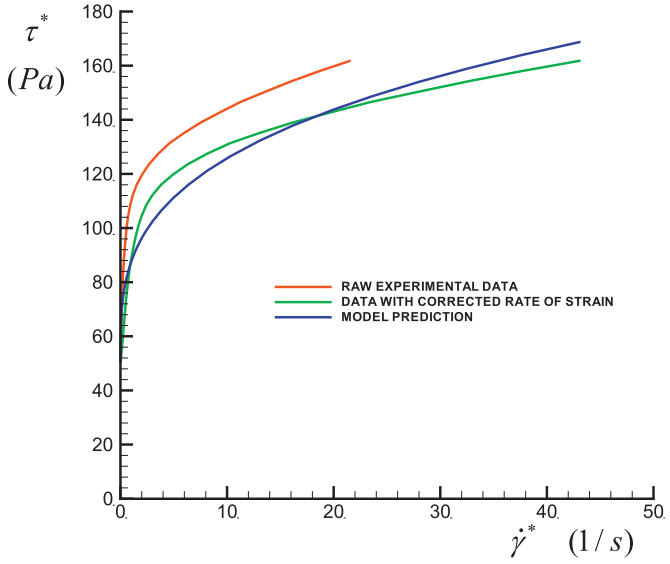

Fig. 9. Comparison of the rheological curves for a cosmetic emulsion. The upper curve (in red) was obtained using the traditional apparent values for the rate of strain while the green curve was obtained using the true (i.e. corrected) values. The blue line, corresponds to the Herschel–Bulkley model with fitted rheological parameters. (For interpretation of the references to colour in this figure legend, the reader is referred to the web version of this article.)

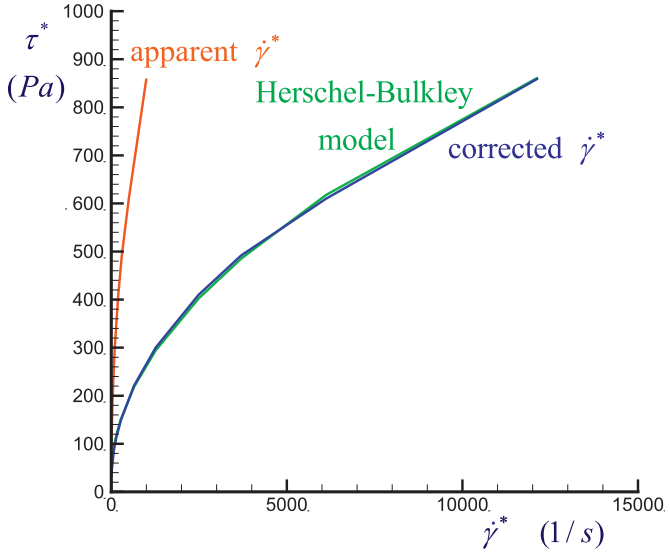

Fig. 10. Comparison of the rheological curves for a coal-water suspension. The upper curve (in red) was obtained using the traditional apparent values for the rate of strain while the lower curve (in blue) was obtained using the true (i.e. corrected) values. The green line, which essentially coincides with the blue line, corresponds to the Herschel–Bulkley model with fitted rheological parameters. (For interpretation of the references to colour in this figure legend, the reader is referred to the web version of this article.)

error when using respectively the corrected and the raw data. The comparison shows a big difference between the apparent values and the true values for the consistency index and the exponent. These results are, of course, consistent with the theoretical predictions of [1].

As a final check, we consider rheological data for a coal-water suspension (with particle diameter 100 μm and mass solid fraction approximately 50%) at a temperature of 20°C, obtained with the same rheometer with a larger gap ($R_1^* = 10$ mm, $R_2^* = 13$ mm, and $L^* = 20$ mm). To avoid slip, the inner cylinder was grooved. Fig. 10 shows the difference between the results obtained from the rheometer (red line) using the traditional apparent values for the rate of strain and those obtained using the true values; the blue line corresponds to the experimental data and the green line to the data obtained using the Herschel–Bulkley model equation (Eq. (3)) with the parameters obtained using the true values of the rate of strain. Fig. 10 shows clearly the large deviation between the experimental data when the apparent values are used. Here, the curve fitting is obtained using non-linear least square analysis for the parameters k and n. Again, the yield stress is obtained independently by linear extrapolation of the lowest two values of the stress. As mentioned above the curve fitting for Fig. 10 was obtained using least square fit and solving the linearized form of the Herschel–Bulkley model by taking the log of the model equation. By comparison we clearly conclude that the non-linear curve fitting yields better results.

For both cases of experimental data considered here, i.e. for the cosmetic emulsion and the coal-water suspension, the rheological parameter that is affected most is the consistency index; the power-law exponent is affected to a less extent, while the yield stress is essentially unaffected.

6. Conclusions

The circular Couette flow used to determine material constants of Herschel–Bulkley fluids has been revisited. It has been established that in order to determine the material constants from rheological data it is of crucial importance to use “true” values for the rate of strain using the constitutive model used to describe the rheology and not Newtonian approximations. It has been also demonstrated that the rate-of-strain distributions across the gap share a common point only in fully-yielded Bingham plastic flows. However, if the gap is sufficiently small the common point for the fully-yielded Bingham case provides a good approximation for determining the material constants in other cases, e.g., for partially-yielded Bingham plastics or fully-yielded Herschel–Bulkley materials. This justifies the common-point concept originally presented by Schümmer and Worthoff [3].

As pointed out by an anonymous referee, since the calibration of a Couette rheometer is based on "standard fluids", as is the case in most experimental processes, the experimental values of the rheological parameters are useful on a relative basis and this relative information is accurate. Finally, it should be underlined that the present analysis does not apply (i.e., it is not necessary) in other rheometric set-ups, e.g. in cone-and-plate rheometry, where the rate of strain is constant.

Acknowledgement

The authors are grateful to the anonymous referees for their constructive comments and criticism.

References

[1] M. Chatzimina, G. Georgiou, A. Alexandrou, Wall shear rates in circular Couette flow of a Herschel – Bulkley fluid, Appl. Rheol. 19 (2009) 34288 2.
[2] A. Alexandrou, G. Georgiou, D. Apelian, Parameter estimation for thixotropic semi–solid slurries, Sol. St. Phenomena. 116-117 (2006) 429–432.
[3] P. Schümmer, R.H. Worthoff, An elementary method for the evaluation of a flow curve, Chem. Eng. Sci. 33 (1978) 759–763.
[4] "German Norm, DIN 53019-1 Measurement of viscosities and flow curves by means of rotational viscometers, Beuth Verlag GmbH 10772 (2009).